Observables for the $pd \to {}^3\mathrm{H}\pi^+$ and $pd \to {}^3\mathrm{He}\pi^0$ reactions in a $pp \to d\pi^+$ model

W. R. Falk
Department of Physics, University of Manitoba, Winnipeg, Manitoba, Canada R3T 2N2
(Received 27 September 1999; published 16 February 2000)

Differential cross sections and spin observables A_y, iT_{11}, T_{20}, and T_{22} are calculated for the $pd \to {}^3\mathrm{H}\pi^+$ reaction in a $pp \to d\pi^+$ model at energies near threshold. The results are compared with experimental data for the reactions $\vec{p}d \to {}^3\mathrm{He}\pi^0$ and $\vec{d}p \to {}^3\mathrm{He}\pi^0$. Good agreement of these predictions with the data for the proton analyzing powers is obtained, and for most of the other observables satisfactory agreement is found. Effects of various assumptions in the model are investigated and discussed.

PACS number(s): 25.40.Qa, 25.10.+s, 21.45.+v, 24.70.+s

I. INTRODUCTION

Understanding pion production in the three nucleon $p+d$ system is important since it represents a level of complexity next to that of the elementary $NN \to NN\pi$ reaction. Effects of the nuclear environment may begin to manifest themselves at this level which has major implications for dealing with $A(p,\pi^+)B$ reactions. Since the wave functions of the light nuclei ^{2}H, ^{3}H, and ^{3}He are well understood, it is to be hoped that a theoretical treatment in the three nucleon sector would be possible. Pion production in the $p+d$ system may well also be important in understanding η production in $p+d$ collisions, where the former may act in an intermediate step [1]. Interpreting double pion production in $p+d$ collisions is another area where the single pion production process must first be understood.

In general, theoretical descriptions of $pd \to X\pi$ reactions have not been particularly successful, despite great efforts by many groups over the years. References to this earlier work, including some of the experimental results, can be found in Canton *et al.* [2]. In order to circumvent many of the problems that beset fully microscopic model calculations Germond and Wilkin [3] introduced experimental amplitude data from the $pp \to d\pi^+$ reaction into the three nucleon sector. They were able to obtain a rather good description of the energy dependence of the forward and backward differential cross section and tensor analyzing power T_{20} using a collinear geometry. Their results near the threshold of the reaction are particularly successful. At energies near threshold the reaction occurs in a kinematic regime where it may be viewed as proceeding via the elementary $NN \to NN\pi$ reaction. Extending this general idea to the case of a three body final state, Meyer and Niskanen [4] analyzed the total cross section for the $pd \to pd\pi^0$ reaction under the assumption that it arises entirely from the quasifree elementary process $pn \to d\pi^0$. They obtained a very good description of the total cross section data of Rohdjess *et al.* [5] when final state interactions were included.

A phenomenological $pp \to d\pi^+$ model developed recently [6] was previously applied to the general case of $A(p,\pi^+)B$ reactions, for predicting differential cross sections and analyzing powers. Here this model is used, with only minor modifications, to make predictions of the numerous experimental observables measured for the $pd \to {}^3\mathrm{He}\pi^0$ reaction near threshold. Although the model specifically calculates observables for (p,π^+) reactions, via the $pp \to d\pi^+$ process, it can also be used to calculate observables for the π^0 reaction, provided that the elementary $pn \to (pn)\pi^0$ process occurs primarily through the NN isospin transition $1 \to 0$. The formalism presently makes no provision for including the d^*, which would then also allow an NN isospin transition $1 \to 1$. Nevertheless, near threshold it is expected that the d^* contribution will be quite small. On the other hand, Germond and Wilkin [3] find this contribution to be especially significant very close to threshold.

Experimental measurements near threshold for the $\vec{d}p \to {}^3\mathrm{He}\pi^0$ reaction have been carried out by Nikulin *et al.* [7]. Their analysis presents differential cross sections and the polarization observables iT_{11}, T_{20}, and T_{22} for 20 energies for pion c.m. momenta ($\eta = p_\pi/m_\pi c$) $0.022 \leqslant \eta \leqslant 0.389$. Differential cross sections and proton analyzing powers for the $\vec{p}d \to {}^3\mathrm{He}\pi^0$ have been measured near threshold in two different experiments at IUCF by Pickar *et al.* [8] and Warman [9]. No experimental data near threshold exist for the $pd \to {}^3\mathrm{H}\pi^+$ reaction.

II. MODEL

The model is described in detail in Ref. [6]; it was modified only to include calculation of the deuteron tensor analyzing powers from the reaction amplitudes. A brief overview, pertinent to the present discussion, is presented here in the context of the $A(p,\pi^+)B$ reaction. An incoming proton with momentum $\vec{k}_p$ [in the $(p+A)$ center-of-mass (c.m.) system] interacts with a target proton of momentum $\vec{k}_0$ producing a pion with momentum $\vec{k}_\pi$, and an associated deuteron. This deuteron recombines with the recoil nucleus to form the final nucleus B. All interactions are treated as local. In a plane wave representation the relative momentum $\vec{q}$ of this deuteron with respect to the recoil nucleus is given by

$$\vec{q} = \left(\frac{A-1}{A}\right)\vec{k}_p + \vec{k}_0 - \left(\frac{A-1}{A+1}\right)\vec{k}_\pi . \tag{1}$$

The recoil nucleus is assumed to be on shell. [For the $pd \to {}^3\mathrm{H}\pi^+$ reaction at 211 MeV or 4.2 MeV (lab) above threshold, $k_p = 422$ MeV/c and $k_\pi = 27$ MeV/c.] From the energies and momenta of the two interacting protons, all the

TABLE I. Low energy amplitudes for the $pp \to d\pi^+$ reaction.

l_π	Amplitude ($mb^{1/2}$)	Phase (deg)
0	$\lvert a_1\rvert = 0.86\eta^{1/2}$	−6.0
1	$\lvert a_0\rvert = 0.086\eta^{3/2}$	−26.8
1	$\lvert a_2\rvert = 2.15\eta^{3/2}$	9.6
2	$\lvert a_6\rvert = 0.52\eta^{5/2}$	−2.9

requisite kinematical quantities in the pp c.m. frame (i.e., the relative momentum $\vec{k}_{pp}$ of the two protons) can be calculated. However, since the $pp \to d\pi^+$ reaction occurs in a nuclear environment, the process is off shell. Indeed, the momenta $\vec{k}_{pp}$ and $\vec{k}_\pi$ are not compatible with the free $pp \to d\pi^+$ process. As described in Ref. [6], it was determined empirically that the overall most satisfactory description was obtained when (1) the angle between the vectors $\vec{k}_{pp}$ and $\vec{k}_\pi$ was used as the pion scattering angle for evaluation of the $pp \to d\pi^+$ reaction amplitudes and (2) the dynamical parameter that defined the energy at which the $pp \to d\pi^+$ reaction amplitudes were evaluated was specified by $\vec{k}_\pi$. Specifically, $\vec{k}_\pi$, the pion momentum in the $(p+A)$ c.m. frame, was also taken as the pion momentum in the free $pp \to d\pi^+$ reaction. Consequently, the energy at which the $pp \to d\pi^+$ reaction amplitudes are evaluated is constant at a given bombarding energy for the $A(p,\pi^+)B$ reaction, independent of $\vec{k}_0$ and of angle.

The momentum distribution of the struck nucleon is important since this defines the momentum distribution of q in the final nuclear state. In the present case the (target) deuteron wave function was taken from Machleidt *et al.* [10]. Inclusion of the D state was found to be very important, as will be shown later. For reasons of analytical simplicity a very simple form for the ^{3}H wave function was employed. Indeed, the relative motion wave function of $(n+d)$ was calculated in an harmonic oscillator (HO) basis, the asymptotic region modified by attaching an asymptotic wave function characteristic of the appropriate separation energy and angular momentum L. This composite wave function was then expanded in an HO basis. From Eq. (1) the magnitude of the momentum q [the relative momentum of $(n+d)$] is about 200 MeV/c. Indeed, the important range for this quantity is more like $\approx$100–200 MeV/c. In this interval the above wave function describes the momentum distribution in ^{3}H, given in Ref. [11], reasonably well.

Low energy parameters for the $pp \to d\pi^+$ reaction have been measured by Korkmaz *et al.* [12], and more recently by Drochner *et al.* [13] and Heimberg *et al.* [14]. While there is some disagreement in the normalization of these different experiments a representative set of amplitudes was extracted from these results for the lowest pion partial waves. These are given in Table I, and follow the definitions used in Ref. [15].

In comparing $pn \to d\pi^0$ and $pp \to d\pi^+$ reactions one must first of all take into account the different masses of the particles involved (principally the different pion masses). This is effectively accomplished by making the comparison at the same values of the pion c.m. momenta. In addition, for the π^+ reaction, Coulomb effects are present. The dependence of the total cross sections near threshold have the form [16]

$$\sigma_{tot}(pp \to d\pi^+) = \alpha C_0^2 \eta + \beta C_1^2 \eta^3,$$

$$\sigma_{tot}(np \to d\pi^0) = \tfrac{1}{2}(\alpha\eta + \beta\eta^3),$$

where the C's are Coulomb correction factors and the factor of 1/2 arises from the isospin Clebsch-Gordan coefficient. In light of the discussion under point (2) above and the total cross section dependences of the elementary $NN \to NN\pi$ reactions, the following criterion was adopted for selecting matching pion momenta in the $pd \to X\pi$ reactions: $C_0^2 \eta_{\pi^+} = \eta_{\pi^0}$. The parametrization of the Coulomb correction factor given in [16] was used. Table II shows that experimental measurements for the $\vec{p}d \to {}^3\mathrm{He}\pi^0$ and $\vec{d}p \to {}^3\mathrm{He}\pi^0$ reactions have been made at very similar values of η_{π^0} in a number of cases. An average value of η_{π^+}, calculated according to the above prescription, is shown in column 5 of Table II. The corresponding proton bombarding energies used in the calculations for the $pd \to {}^3\mathrm{H}\pi^+$ reaction are shown in column 6.

TABLE II. Bombarding energies (lab) and pion (c.m.) momenta.

$\vec{p}+d \to {}^3\mathrm{He}+\pi^0$		$\vec{d}+p \to {}^3\mathrm{He}+\pi^0$		$p+d \to {}^3\mathrm{H}+\pi^+$	
T_p (MeV)	η_{π^0}	T_d (MeV)	η_{π^0}	η_{π^+}	T_p (MeV)
199.4	0.079	398.75	0.082	0.099	207.9
200.5	0.127	400.75	0.126	0.145	209.2
202.1	0.175			0.192	211.0
		405.75	0.197	0.214	212.0
205.0	0.240	409.75	0.239	0.256	214.2
210.0	0.323	419.75	0.322	0.337	219.5
		429.75	0.389	0.402	224.8

III. RESULTS

A. Near threshold

Calculations for all the observables for the $pd \to {}^3\mathrm{H}\pi^+$ reaction were made at the proton bombarding energies shown in Table II. The reference calculations used the $pp \to d\pi^+$ reaction amplitudes given in Table I, a D state component in the wave function for the deuteron target [10] and an S state only ^{3}H final nucleus wave function [6]. Results of these calculations are shown by the solid lines in Figs. 1–5; the number shown in each panel represents the proton bombarding energy shown in the last column of Table II. Experimental data for the $\vec{p}d \to {}^3\mathrm{He}\pi^0$ reaction analyzing powers [9] corresponding to the energies shown in column 1 of Table II are shown in Fig. 2; experimental data for the $\vec{d}p \to {}^3\mathrm{He}\pi^0$ reaction [7] corresponding to the energies shown in column 3 of Table II are shown in Fig. 1 and Figs. 3–5.

Figure 1 shows the differential cross sections where the $pd \to {}^3\mathrm{H}\pi^+$ reaction calculations have been plotted without

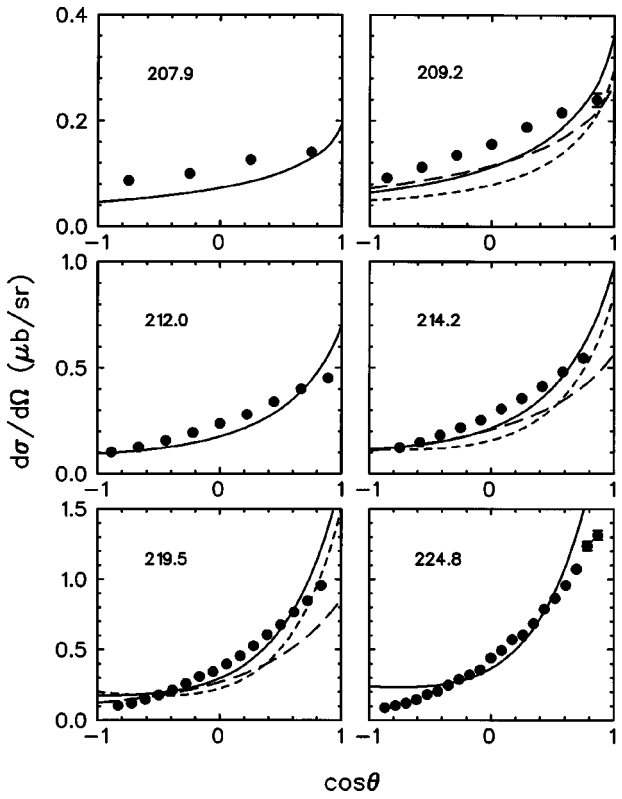

FIG. 1. Differential cross sections for the $pd\rightarrow X\pi$ reaction. The data are from Ref. [7] for the $\vec{d}p\rightarrow{}^3\mathrm{He}\pi^0$ reaction. The calculations are for the $pd\rightarrow{}^3\mathrm{H}\pi^+$ reaction at the energies shown in each of the panels (as specified in Table II). The solid line is for the reference calculation as described in the text; the short dashed lines are calculations where the ^{2}H target wave function is represented by an S state only; the long dashed lines are calculations using the $pp\rightarrow d\pi^+$ reaction amplitude a_1 as given in Table I, and the a_2 amplitude reduced to half its value. For the normalization see explanation in the text.

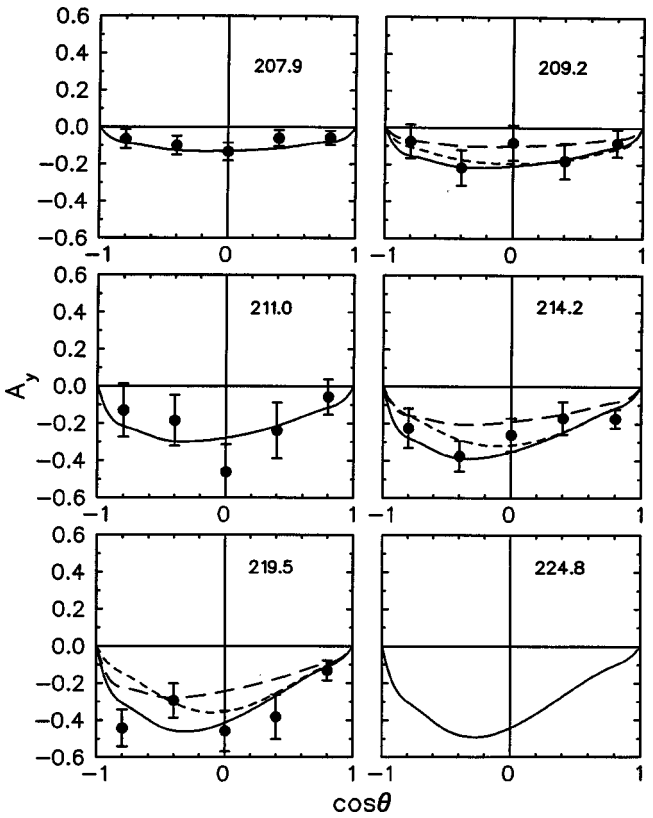

FIG. 2. Analyzing power distributions for the $pd\rightarrow X\pi$ reaction. The data are from Ref. [9] for the $\vec{p}d\rightarrow{}^3\mathrm{He}\pi^0$ reaction. The calculations are for the $pd\rightarrow{}^3\mathrm{H}\pi^+$ reaction at the energies shown in each of the panels (as specified in Table II). Other details are as given in Fig. 1.

any normalization factors applied. However, since an isospin factor (Clebsch-Gordan coefficient) of 1/2 should be applied to this reaction before comparison with the $\vec{p}d\rightarrow{}^3\mathrm{He}\pi^0$ reaction, it is observed that the calculated cross sections are too low by approximately a factor of 2. In general the forward-backward angle asymmetry is somewhat greater in the calculated angular distributions than in the data. Nikulin *et al.* [7] show that near threshold the differential cross sections exhibits scaling as a function of $\eta\cos\theta$. The calculated values from the present model do, indeed, follow this scaling, forming a narrow band with little scatter.

Analyzing power angular distributions are shown in Fig. 2. The calculations fit the data very well, and reproduce the asymmetry about 90° observed at the higher energies. The experimental values of iT_{11} for the $\vec{d}p\rightarrow{}^3\mathrm{He}\pi^0$ reaction shown in Fig. 3 are consistent with zero. The calculations consistently predict positive values, reaching magnitudes as high as ≈ 0.25, which are inconsistent with the data. Angular distributions of T_{20} are shown in Fig. 4. At the lowest two energies the calculations are just slightly more negative than the data, but in good agreement with their general shape. As the energy is increased the calculations tend to show greater forward-backward angle asymmetry and are less negative than the data. The scaling with $\eta\cos\theta$ of the differential cross section was also found to apply to the T_{20} data [7], but with somewhat greater scatter of the data points. This scaling is only approximately followed for the results calculated from the present model. Finally, in Fig. 5 are shown the angular distributions of T_{22}. Both the experimental data and the (reference) calculation are consistent with zero at all angles and energies.

At several selected energies additional calculations were performed in order to test the sensitivities of the calculations to the input parameters. First of all, calculations were performed using only the $pp\rightarrow d\pi^+$ reaction amplitudes a_1 (pion s wave) and a_2 (dominant pion p wave). These results were essentially indistinguishable from the reference calculations for all observables at all energies. Thus the pion d wave does not appear to be significant at these low energies and the p-wave amplitude a_0 is small compared with the a_2 amplitude. Next, calculations were performed using only the amplitude a_1. As expected, the observables A_y, iT_{11}, and T_{22} are zero with s-wave pions only; T_{20} assumes the limiting value of $-\sqrt{2}$, and the predicted cross sections are much reduced. An intermediate set of calculations was performed using a_1 and a_2, with the latter amplitude reduced by one-half. These results are shown in Figs. 1–5 by the long dashed lines for selected energies. The reduced p-wave strength re-

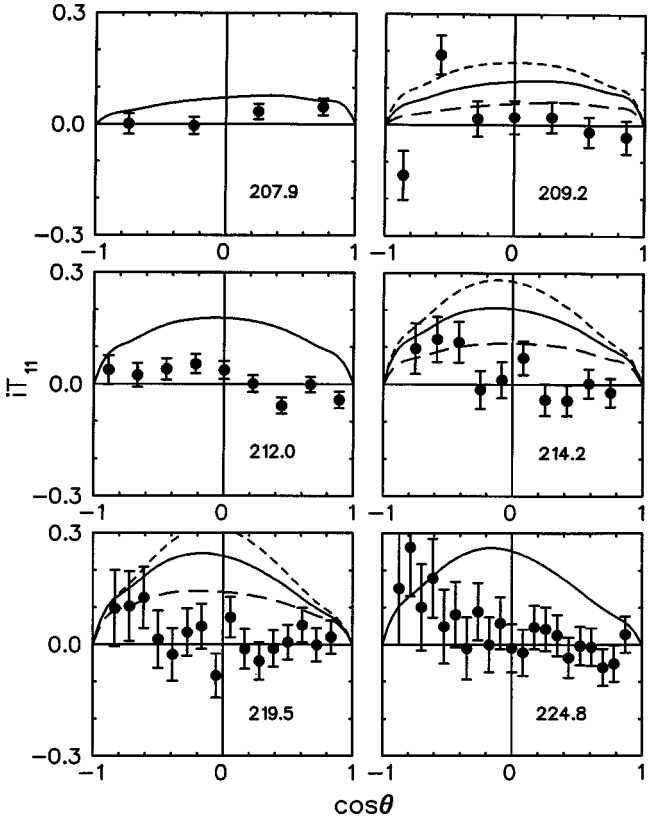

FIG. 3. Angular distributions of iT_{11}. Other details are as given in Fig. 1.

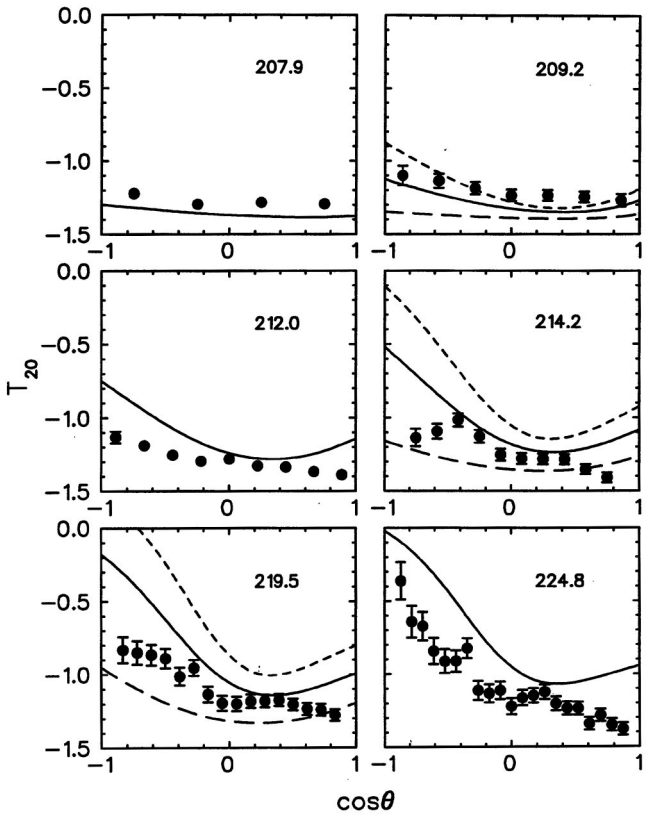

FIG. 4. Angular distributions of T_{20}. Other details are as given in Fig. 1.

sults in flatter angular distributions for the differential cross sections (Fig. 1), underestimating the forward-backward angle asymmetry. Also, as expected, the analyzing powers (Fig. 2) become much shallower, which is inconsistent with the data. The values of iT_{11} are reduced to about half of the value of the earlier calculations (Fig. 3), and the T_{22} values remain consistent with zero (Fig. 5). For T_{20} the forward-backward angle asymmetry is much reduced and the values are more negative, now generally falling below the data.

Additional calculations were also performed to examine the effects of *D* state components in the wave functions of ^{2}H and ^{3}H. When a *D* state component for ^{3}H was included, as well as for ^{2}H (reference calculation), the results generally showed no improvement for the various observables at the different energies. However, if an *S* state wave function was used for ^{2}H as well as for ^{3}H, the results were in poorer agreement with the data for all observables. These results are shown by the short dashed line in Figs. 1–5. The presence of higher momentum components in the target wave function thus appears to be more important than in the final nucleus. Possible explanations for this behavior are discussed in Sec. IV.

B. Higher energies

Some further investigations at energies well above threshold were also carried out. Previous results for calculations of the differential cross sections and analyzing powers for the $pd \rightarrow {}^3\mathrm{H}\pi^+$ reaction using this model have been reported [6] in the energy range from 250 to 500 MeV. These calculations used the full amplitude set for the $pp \rightarrow d\pi^+$ reaction from the data of Bugg *et al.* [18], as discussed in Ref. [6]. As a check on these amplitudes calculated differential cross sections and analyzing powers for the $pp \rightarrow d\pi^+$ reaction were compared with those obtained from SAID [19] using the phase shift solution SP94. The results are compared in Table II of Ref. [20]; the agreement is very good.

A general feature of the calculated analyzing powers for $pd \rightarrow {}^3\mathrm{H}\pi^+$ in the range from 277 to 350 MeV is that they are considerably less negative at the minimum than the experimental data. At 500 MeV they are in strong disagreement with the data. On the other hand, the shape of the differential cross sections is quite well reproduced, but their magnitudes are too large by a factor of $\approx$2.6. This observation on the normalization for the differential cross sections also applies to the 0° and 180° data of Kerboul *et al.* [17] for the $\vec{d}p \rightarrow {}^3\mathrm{He}\pi^0$ reaction for deuteron bombarding energies of 500–790 MeV. Kerboul *et al.* [17] also report tensor analyzing powers T_{20} at 0° and 180° for the same reaction. Combining these data with those of Nikulin *et al.* [7] reveals that from 400 to 790 MeV the 0° data for T_{20} increase monotonically from a value of ≈ -1.4 to ≈ -0.9. The calculated values at the equivalent bombarding energies for the $pd \rightarrow {}^3\mathrm{H}\pi^+$ reaction rise rapidly from a value of -1.4 to a value of ≈ -0.6 at 500 MeV, and remain relatively constant at this value up to 790 MeV. At 180° the T_{20} data rise very rapidly from a value of ≈ -1.2 at 400 MeV to ≈ -0.2 at

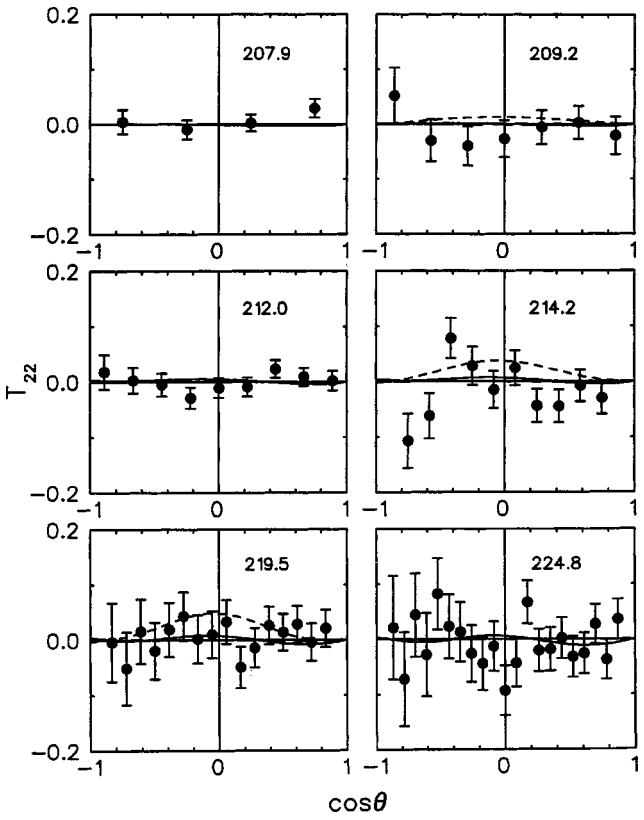

FIG. 5. Angular distributions of T_{22}. Other details are as given in Fig. 1.

450 MeV, and then decrease smoothly once more to ≈ -1.3 at 670 MeV. The calculated values show this rapid rise, but a more gradual dropoff thereafter.

IV. DISCUSSION

A $pp \rightarrow d\pi^+$ reaction model has been used to calculate differential cross sections and spin observables for the $pd \rightarrow {}^3\mathrm{H}\pi^+$ reaction, and comparisons made with data from the $\vec{p}d \rightarrow {}^3\mathrm{He}\pi^0$ and $\vec{d}p \rightarrow {}^3\mathrm{He}\pi^0$ reactions. Near threshold, *s*-wave and *p*-wave pions are sufficient in describing the data; inclusion of *d*-wave pions has negligible effects on the results. The differential cross section displays scaling as a function of $\eta \cos\theta$, as observed in Ref. [7]. On the other hand, for T_{20} this scaling is only approximately followed in the model. For the differential cross sections the calculated forward-backward asymmetry is somewhat greater than observed in the data. This asymmetry can be reduced by reducing the pion *p*-wave amplitude, that is, by reducing the angular dependence of the underlying $pp \rightarrow d\pi^+$ reaction. The asymmetry also depends on the momentum distributions in ^{2}H and ^{3}H. The magnitudes of the cross sections are underestimated by approximately a factor of 2. (At higher energies the cross sections are overestimated.)

Analyzing power data are very well described by this model, requiring the full *s*-wave and *p*-wave amplitudes as determined by independent low energy measurements for the $pp \rightarrow d\pi^+$ reaction. Any reduction in the *p*-wave amplitude results in less negative values of the analyzing powers. On the other hand, a reduction in the *p*-wave amplitude would result in a better fit to the T_{20} data. The reference calculations reproduce the shapes of the T_{20} distributions quite well, although they are generally shifted to somewhat more positive values than observed experimentally. Likewise, the iT_{11} data would prefer a smaller value of the *p*-wave amplitude, to yield values closer to the experimental values that are consistent with zero. Perhaps these observations suggest that the use of the on-shell $pp \rightarrow d\pi^+$ amplitudes affects the different observables in different ways, and only a more rigorous calculation can account for these effects.

The reference calculations used a *D* state component in the ^{2}H target wave function but not in the residual ^{3}H wave function. However, using an *S* state component only in the ^{2}H wave function resulted in much inferior fits to all the observables. Much less sensitivity in the calculations was observed for the ^{3}H *D* state strength compared with the ^{2}H *D* state strength. A possible explanation for this may be due to the fact that in the pertinent momentum intervals for the target and residual nucleus the relative *D* state to *S* state momentum strength in the deuteron is much greater than in ^{3}H. On the other hand, Germond and Wilkin [3] in their calculation find a *D* state component in the residual nucleus, as well as the target, to be important. Their inclusion of nonlocal effects may well enhance the relative contribution from the *D* state component in the residual nucleus. The use of a better ^{3}H wave function in the present model would undoubtedly change the sensitivity of observables to the *D* state strength; however, it is not expected that the main conclusions would be altered significantly.

Experimental values of T_{22}, as for iT_{11}, are consistent with zero for all energies and angles. The calculations for T_{22} are in agreement with this, with the exception of the calculations that do not include a *D* state component in ^{2}H; these exhibit small, but non-negligble positive values. For iT_{11}, all calculations yield significant positive values, in disagreement with the data. Indeed, the predictions give $iT_{11} \approx -0.5A_y$. In an attempt to understand this relationship the observables iT_{11} and A_y were expressed in terms of the partial cross sections calculated in a transverse (or Madison) frame. Although some of these partial cross sections are quite small, relative to others, there is no simple relationship that can be deduced from this comparison as to the value of the above ratio.

One possible shortcoming of this model is that in the elementary $pp \rightarrow pn\pi^+$ process only the isoscalar final nucleon pair is taken into account. Germond and Wilkin [3] show that the forward angle differential cross sections and T_{20} values are sensitive to the isovector d^* contribution in their model. Indeed, the forward angle T_{20} values as a function of energy predicted by this model are qualitatively very similar to their results when they use the isoscalar amplitudes alone. At backward angles they find little difference in calculations that use isoscalar amplitudes only and those that use isoscalar plus isovector amplitudes. The predictions of the present model fall midway between their results. For the differential cross section, on the other hand, better agreement at forward angles is observed between the models when comparing with their isoscalar plus isovector calculation.

The role of the isovector d^* contribution thus remains to be clarified.

Another shortcoming of the model relates to the rather arbitrary and empirical manner used in defining the pion scattering angle and pion energy at which the amplitudes for the $pp \to d\pi^+$ reaction were evaluated. Nevertheless, despite these limitations, this simple model based on the underlying $pp \to d\pi^+$ mechanism has demonstrated the ability to correlate a sizable body of diverse experimental data. Recent calculations for the $pd \to {}^3\mathrm{H}\pi^+$ reaction that deal with pion production in the three nucleon system from a much more rigorous approach are presented by Canton *et al.* [2].

ACKNOWLEDGMENTS

The author is grateful to L.K. Warman for permission to use his analyzing power data prior to publication. This work was supported in part by the Natural Sciences and Engineering Research Council of Canada.

[1] G. Fäldt and C. Wilkin, Nucl. Phys. **A587**, 769 (1995).
[2] L. Canton, G. Cattapan, G. Pisent, W. Schadow, and J. P. Svenne, Phys. Rev. C **57**, 1588 (1998); L. Canton and W. Schadow, *ibid.* **56**, 1231 (1997).
[3] Jean-Francois Germond and Colin Wilkin, J. Phys. G **16**, 381 (1990); **14**, 181 (1988).
[4] H. O. Meyer and J. A. Niskanen, Phys. Rev. C **47**, 2474 (1993).
[5] H. Rohdjess *et al.*, Phys. Rev. Lett. **70**, 2864 (1993).
[6] W. R. Falk, Phys. Rev. C **50**, 1574 (1994).
[7] V. N. Nikulin *et al.*, Phys. Rev. C **54**, 1732 (1996).
[8] M. A. Pickar, A. D. Bacher, H. O. Meyer, R. E. Pollock, and G. T. Emery, Phys. Rev. C **46**, 397 (1992).
[9] L. K. Warman, Ph.D. thesis, Indiana University, 1998; Phys. Rev. C (submitted).
[10] R. Machleidt, K. Holinde, and Ch. Elster, Phys. Rep. **149**, 1 (1987).
[11] R. Schiavilla, V. R. Pandharipande, and R. B. Wiringa, Nucl. Phys. **A449**, 219 (1986).
[12] E. Korkmaz, Jin Li, D. A. Hutcheon, R. Abegg, J. B. Elliott, L. G. Greeniaus, D. J. Mack, C. A. Miller, and N. L. Rodning, Nucl. Phys. **A535**, 637 (1991).
[13] M. Drochner *et al.*, Phys. Rev. Lett. **77**, 454 (1996).
[14] P. Heimberg *et al.*, Phys. Rev. Lett. **77**, 1012 (1996).
[15] B. Blankleider and I. R. Afnan, Phys. Rev. C **31**, 1380 (1985).
[16] D. A. Hutcheon *et al.*, Nucl. Phys. **A535**, 618 (1991).
[17] C. Kerboul *et al.*, Phys. Lett. B **181**, 28 (1986).
[18] D. V. Bugg, A. Hasan, and R. L. Shypit, Nucl. Phys. **A477**, 546 (1988); D. V. Bugg, *ibid.* **A437**, 534 (1985); R. A. Arndt, I. I. Strakovsky, R. L. Workman, and D. V. Bugg, Phys. Rev. C **48**, 1926 (1993), and references therein.
[19] R. A. Arndt, Scattering analysis interactive dial-in program SAID (unpublished).
[20] R. G. Pleydon *et al.*, Phys. Rev. C **59**, 3208 (1999).